

Journal of Materials Chemistry A

Accepted Manuscript



This is an *Accepted Manuscript*, which has been through the Royal Society of Chemistry peer review process and has been accepted for publication.

Accepted Manuscripts are published online shortly after acceptance, before technical editing, formatting and proof reading. Using this free service, authors can make their results available to the community, in citable form, before we publish the edited article. We will replace this *Accepted Manuscript* with the edited and formatted *Advance Article* as soon as it is available.

You can find more information about *Accepted Manuscripts* in the [Information for Authors](#).

Please note that technical editing may introduce minor changes to the text and/or graphics, which may alter content. The journal's standard [Terms & Conditions](#) and the [Ethical guidelines](#) still apply. In no event shall the Royal Society of Chemistry be held responsible for any errors or omissions in this *Accepted Manuscript* or any consequences arising from the use of any information it contains.

ARTICLE

Polypropylene Elastomer Composite for the All-Vanadium Redox Flow Battery: Current Collector Materials

Cite this: DOI: 10.1039/x0xx00000x

Received 00th January 2012,
Accepted 00th January 2012

DOI: 10.1039/x0xx00000x

www.rsc.org/

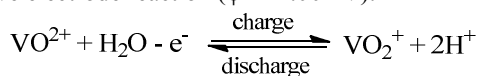
Jihai Zhang,^a Tao Zhou,^{a,*} Liping Xia,^a Canyao Yuan,^b Weidong Zhang,^b and Aiming Zhang^{a,*}

In this study, carbon-based polypropylene thermoplastic elastomer (PP-elastomer) composite for current collectors of all-vanadium redox flow battery (VRB) was successfully prepared. The volume resistivity of the PP-elastomer composite was 0.47 $\Omega \cdot \text{cm}$. Its tensile strength and elongation at break were 6.6 MPa and 250%, respectively. In addition, good flow property in processing makes this composite has the potential on mass industrial production of current collectors. The single cell and the cell stack of VRB battery equipped with the composite current collectors were assembled for battery tests, including cyclic voltammetry, long-term performance, long-term stability, and the oxidation corrosion. To evaluate the stability and the performance of the cell stack under a long-term operating condition, tests with more than 2300 charge-discharge cycles were carried out. The coulombic efficiency (CE) and voltage efficiency (VE) of the cell stack maintained around 93% and 80% during 2300 charge-discharge cycles, and energy efficiency EE hold around 75%. The results approved that VRB battery equipped the composite current collectors had a good stability and performance. Furthermore, long-term corrosion tests indicated that PP-elastomer composite could endure the strong corrosion of pentavalent vanadium and the concentrated sulfuric acid. The composite materials prepared in this study are more suitable to produce the current collectors. The corrosion resistance of composite materials is much better than that of the graphite, and the mechanism was also discussed.

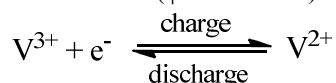
1. Introduction

Recently, there has been increasing interest in the all-vanadium redox flow battery (VRB) due to its long cycle life and high energy efficiencies.¹⁻¹¹ In historic perspective, the earliest comprehensive and systematic study on VRB is Skyllas Kazacos (University of New South Wales, Australia) in the 1980s.¹²⁻¹⁵ Figure 1 illustrates the simple schematic of the VRB system,¹⁶ wherein the cell stack is the core of VRB. The cell stack consists of electrodes (including graphite felts and current collectors), the electrolyte, separator (proton exchange membrane),¹⁷⁻²⁰ and seals. In the VRB system, the $\text{VO}^{2+}/\text{VO}_2^+$ and $\text{V}^{3+}/\text{V}^{2+}$ redox couples are employed for the positive and negative half-cells, respectively. The electrochemical reactions during charge-discharge process were listed as follows:²¹⁻²³

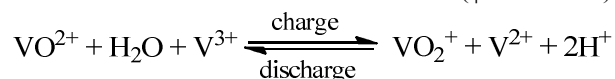
Positive electrode reaction ($\varphi^0 = 1.004 \text{ V}$):



Negative electrode reaction ($\varphi^0 = -0.255 \text{ V}$):



Overall electrochemical reaction of the cell ($\varphi^0 = 1.259 \text{ V}$):



All-vanadium redox flow battery has a capacity on theoretically unlimited charging and discharging, which is superior to other types of batteries. However, excessive overcharging of the VRB can lead to degradation of the positive electrode and decreases the cycle life. The most critical issue for the development of VRB is the identification, characterization, and fabrication of suitable electrode materials with low cost, light weight, flexibility, and good stability under highly corrosive operating conditions,²¹ especially for current collector materials. To date, several kinds of carbon-based electrode materials have been investigated for VRB application.²⁴ Graphite felt is an ideal VRB electrode material which provided active sites for the vanadium redox reaction due to its higher specific surface areas and enhanced three-dimensional network structures, excellent conductivity, and electrochemical stability.²⁵ Moreover, through surface treatments such as chemical etching,²⁶ nanoparticle decorating,^{27, 28} thermal treatment,²⁹ the electrochemical reaction kinetics on graphite felt will be greatly improved.

According to the literature, there also have been several laboratory studies on the current collector materials with different materials. The gold, lead, platinum, titanium and titanium-based battery electrode as the current collector were investigated.²¹ It was found that the platinum electrode was easy to form a surface oxide film in H_2SO_4 solution, and the gold or the lead electrode had a poor electrically chemistry reversibility for the $\text{VO}_2^+/\text{VO}^{2+}$ redox couple. Furthermore, the anode region tended to generate the passivation film and hindered the electrochemical reaction. By contrast, the conductive carbon-polymer composite has become an attractive alternative for the VRB current collector materials in recent years due to its excellent performance.^{15, 29-34} Zhong et al³⁰ investigated a conductive polyethylene composite with a high electrochemical activity and stability. It was observed that the composite modified by high content of carbon fiber could further improve electrode activity. The pioneer work of the conductive carbon-polymer composite based on polypropylene (PP) for VRB was reported by Haddadi-Asl et al.^{31, 32} They successfully fabricated composite materials based on rubber (EPR, EPDM, and SEBS) modified PP, and it was found that the mechanical property of high-density polyethylene (HDPE) was better than PP. However, the electrical conductivity of HDPE was inferior to that of PP. Kazacos et al¹⁵ studied a polyethylene composite filled by the graphite powder which demonstrated that high-energy efficiencies can be achieved with the vanadium redox cell employing electrodes consisting of graphite felt bonded onto carbon plastic sheets as the current collector. Caglar et al³⁵ developed a carbon nanotube and graphite filled polyphenylene sulfide based bipolar plates, which had high electrical conductivities and mechanical properties.

However, the conductivity of the carbon-plastic composite was much less than that of graphite materials. As far as we knew, the electrolyte of VRB has a strong oxidizing during the charge-discharge process.¹²⁻¹⁴ Unfortunately, currently used polymeric substrate can be probably corroded by oxidation, resulting in the shedding of the conductive filler and the electrical resistance sharply increased during the operation of the vanadium battery.^{31, 36} The widely used graphite current collectors also appear obvious corrosion phenomena in the course of the charge-discharge process. This corrosion for current collector materials is a potential danger to the leakage accident of VRB. In spite of this fact, few studies have focused on this issue to date. Therefore, developing a convenient and low-cost current collector materials for VRB on a large scale will be urgent and of great importance.²⁴

The purpose of the present study is to develop a kind of the current collector materials based on a novel polypropylene thermoplastic elastomer (PP-elastomer) composite for VRB. This PP-elastomer is a novel copolymer of vinyl monomers and propylene monomers, which is synthesized via a metallocene catalyst with a small amount of vinyl monomers randomly inserting in the main chain of polypropylene. In the pioneer work of Haddadi-Asl et al.,^{31, 32} the polymer matrix of carbon-polymer composites was rubber modified PP, whereas the matrix of the prepared composites in the present study is a novel thermoplastic elastomer with an excellent toughness and processability. The prepared composite in this study has a lower volume resistivity ($0.47 \Omega \cdot \text{cm}$) and good mechanical properties (tensile strength: 6.6 MPa; elongation at break: 250%). In addition, this composite has the potential on mass industrial production of current collectors due to its outstanding flow property in processing. We confirm that VRB with the current

collector of the prepared composite still maintains high-energy efficiency (75%) after more than 2300 charge-discharge cycles. Experiments also show that, as the current collector materials, PP-elastomer composite performs excellent corrosion resistance under the strong oxidation of pentavalent vanadium and concentrated sulfuric acid.

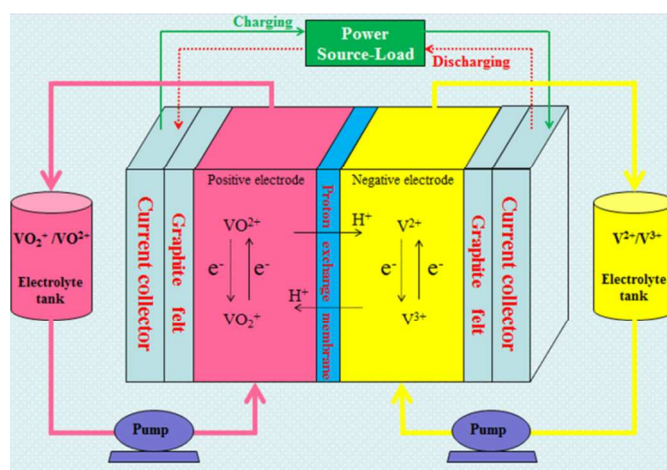


Figure 1. A simple scheme of all-vanadium redox flow battery.

2. Experimental

2.1. Materials

Polypropylene elastomer (PP-elastomer, Vistamaxx 6202, propylene content: 85%; melt flow rate: 7.4 g/10min; density: 0.861 g/cm^3), which was synthesized via a metallocene initiator with a small amount of vinyl monomers randomly inserting in the main chain of polypropylene, was supplied by ExxonMobil Chemical Co. Polypropylene (PP, K8303, melt flow rate: 1.0-3.0 g/10min) was purchased from Beijing Yanshan Petrochemical Co., Ltd. Carbon black (CB, Ensaco350G, extra-conductive) was produced by Timcal Belgium S.A., Switzerland. Carbon fiber (CF, conductive) was bought from Nantong shenyou carbon fiber Co. (China). The average diameter of the carbon fiber was $7 \mu\text{m}$, and its length was 5-6 mm. The vanadium electrolyte (SDY-6) was supplied by Panzhihua Iron and Steel Research Institute. All the materials were used as received without any further treatment.

2.2. Preparation of composites and current collectors

PP-elastomer composite was prepared using a laboratory two-roll mill. The formulations with ingredients are listed in **Table 1**. PP-elastomer was first masticated for 3 min at 80°C , and then polypropylene (PP) was added and continued to masticating for 5 min at 170°C . After that, conductive fillers, such as carbon blacks (CB) and (or) carbon fibers (CF), were added. Masticating was kept for 3 min to ensure a homogeneous distribution of ingredients. The sheets of mixed compounds were taken out of the two-roll mill, and stored at room temperature for 24 h before molding. Finally, the composite current collector was obtained by compression molding in a mold at a pressure of 10 MPa (200°C).

2.3. Treatment for graphite felt

Graphite felt used in the present study was produced by Shanghai Eiki Carbon Co., Ltd. Graphite felt was first immersed in a concentrated HNO_3 solution at 80°C for 5 h, and

Table 1. Formulations and ingredients of polypropylene elastomer composite. The number in brackets is the relative percentage with respect to the total polymer or the total conductive fillers in the composite, which also can be understood as the weight ratio of PP:PP-elastomer or carbon fiber:carbon black.

Ingredients		Content (wt.%)									
PP-elastomer/carbon fiber											
PP-elastomer	90	85	80	75	70	65	60	55	50	45	40
carbon fiber	10	15	20	25	30	35	40	45	50	55	60
PP-elastomer/carbon black											
PP-elastomer	90	85	80	75	70	65	60	55	50	45	40
carbon black	10	15	20	25	30	35	40	45	50	55	60
PP-elastomer/PP/carbon black											
PP-elastomer	85 (100)	76.5 (90)	68 (80)	59.5 (70)	51 (60)	42.5 (50)	34 (40)	25.5 (30)	17 (20)	8.5 (10)	0 (0)
PP	0 (0)	8.5 (10)	17 (20)	25.5 (30)	34 (40)	42.5 (50)	51 (60)	59.5 (70)	68 (80)	76.5 (90)	85 (100)
carbon black	15	15	15	15	15	15	15	15	15	15	15
PP-elastomer/PP/carbon black/carbon fiber											
PP-elastomer	40	40	40	40	40	40	40	40	40	40	40
PP	10	10	10	10	10	10	10	10	10	10	10
carbon fiber	0 (0)	5 (10)	10 (20)	15 (30)	20 (40)	25 (50)	30 (60)	35 (70)	40 (80)	45 (90)	50 (100)
carbon black	50 (100)	45 (90)	40 (80)	35 (70)	30 (60)	25 (50)	20 (40)	15 (30)	10 (20)	5 (10)	0 (0)

then followed by rinsing with deionized water to neutral pH and drying. The purpose of the treatment was the enhancement of its surface hydrophilicity and the generation of a great amount of C–O–H and C=O groups on the surface of graphite fibers.²⁹ These functional groups provided a location for the water adsorption and other polar compounds, and then accelerated the redox reactions of the vanadium species.

2.4. Treatment for proton exchange membrane

Perfluorosulfonic acid proton exchange membrane (GEFC-10N) used in this study was obtained from Beijing Jinneng fuel battery Co., Ltd. The proton exchange membrane was first immersed in water bath with 5 wt.% hydrogen peroxide (H₂O₂) at 80 °C for 60 min, and then was washed with deionized water for five times. After that, the membrane was immersed in 1 mol/L H₂SO₄ solution at 80 °C for 30 min. Finally, it was stored in deionized water until use.

2.5. Characterizations and testing

2.5.1. Volume resistivity

Samples with the volume resistivity higher than 10¹⁰ Ω·cm was measured using a ZC36 Megger (Shanghai Precision Scientific Instruments). Samples with the volume resistivity less than 10² Ω·cm was measured using a 4200-SCS four-point probe instrument (Guangzhou Institute of Semiconductor Material). The volume resistivity between 10²–10¹⁰ Ω·cm was measured using an YD9820A programmable insulation resistance tester (Changzhou Yangtze Electronics), and the test voltage was 10 V.

2.5.2. Cyclic Voltammetry

Cyclic voltammetry of VRB were measured by a LK98B II electrochemical analysis system (Tianjin Orchid Chemical Co., Ltd.) according to triangular wave scan with the potential range between -1.0 V and 2.0 V at scan rate of 0.02 V/s. All potentials were measured using platinum and calomel as the electrode and the reference electrode, respectively. The electrolyte was 1.5 mol/L VOSO₄ and 2.0 mol/L H₂SO₄.

2.5.3. Charge-discharge measurements of VRB

Galvanostatic charge-discharge measurements were controlled by a battery charge-discharge device detection system at 25 °C. For the single cell, the electrode area was 28 cm², and the felt thickness was 5 mm. The thickness of composite current collectors was 5 mm. The half-cell cavity thickness was 3.8 mm. The felt was contact made by contact and compression. To determine the efficiency of the single cell, the charge-discharge measurement of the single cell was performed at the constant current (CC) mode of 70 mA·cm⁻². The effective reaction areas of electrolyte and electrodes were 28 cm². For the single cell, the volume of the anolyte was 100 ml, which contained 1.5 mol/L V³⁺ and 2.0 mol/L total sulphate concentration. At the same time, the volume of the catholyte was also 100 ml, containing 1.5 mol/L V⁴⁺ and 2.0 mol/L total sulphate concentration. For the cell stack, the electrode area was 2000 cm², and other details on cell configuration were the same as the single cell. Then, the charge-discharge measurement of the cell stack was performed at CC mode of 50 mA·cm⁻². The effective reaction areas of electrolyte and electrodes were around 2000 cm². The anolyte contained 1.5 mol/L V³⁺ and 2.0 mol/L total sulphate concentration, and its volume was 16.5 L. The volume of the catholyte was also 16.5 L, containing 1.5 mol/L V⁴⁺ and 2.0 mol/L total sulphate concentration. The coulombic efficiency (CE), voltage efficiency (VE), and energy efficiency (EE) of the VRB were calculated as following equations:³⁷

CE = (A_{discharge} / A_{charge}) × 100% (1)

VE = (V_{m-discharge} / V_{m-charge}) × 100% (2)

EE = CE × VE (3)

where A_{discharge} and A_{charge} are the discharge capacity and the charge capacity, respectively. V_{m-discharge} and V_{m-charge} are the middle point of discharge voltage and charge voltage, respectively.

2.5.4. Scanning electron microscopy (SEM)

SEM micrographs of the surface of current collectors and graphite felts before and after more than 2300

Journal of Materials Chemistry A Accepted Manuscript

charge-discharge processes were observed with JSM-5900LV (Hitachi, Japan) at 20 kV. The samples were coated with a thin layer of gold to reduce charging during observation.

2.5.5. Mechanical test

Tensile properties tests for PP-elastomer composite were performed using molded samples according to ISO 527-1, 2 standards. All tests were performed using a universal testing machine (Instron 4302) at a rate of 200 mm/min. The value of the tensile strength and the elongation were calculated from the average of the test data with 5 times.

2.5.6. Rheological property of the composite

Rheological properties of the PP-elastomer composite were performed using a RosandRH7D high-pressure capillary rheometer at 200 °C. The diameter of capillary die was 1 mm with an aspect ratio 16.

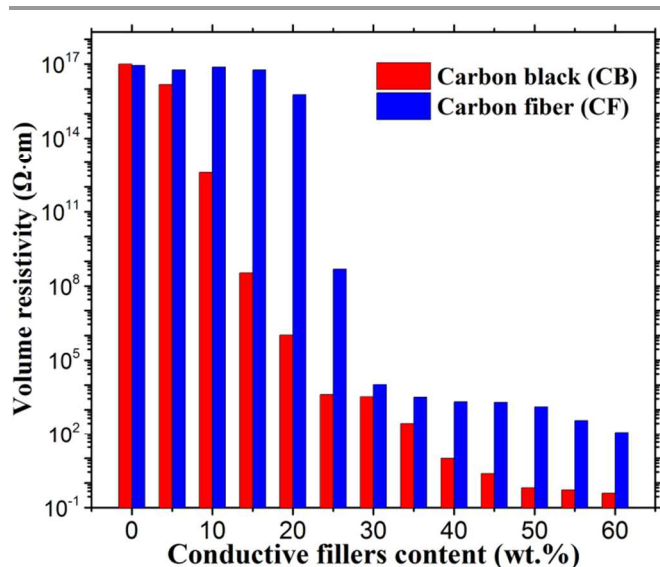


Figure 2. Volume resistivity of PP-elastomer/carbon black and PP-elastomer/carbon fiber composites with different amount of carbon blacks and carbon fibers.

3. Results and Discussion

3.1. Basic properties of polypropylene elastomer composite

Carbon black and carbon fiber have a much great tendency to form a conductive network due to their chain-like or grapes-like aggregate structure.³⁸ The influence of the different amount of the carbon black and carbon fibers on volume resistivity of PP-elastomer/carbon black composite, and PP-elastomer/carbon fiber composite are shown in **Figure 2**. It can be observed that the volume resistivity decreases with the amount of conductive fillers increasing. The percolation threshold of PP-elastomer/carbon black composite and PP-elastomer/carbon fiber composite is around 15-20 wt.% and 20-30 wt.%, respectively. The volume resistivity of PP-elastomer/carbon black composite is significantly lower than that of PP-elastomer/carbon fiber composite when the amount of the conductive filler (carbon blacks or carbon fibers) is above 10 wt.%. Both composites exhibit a transition from an insulator to a conductor with the conductive fillers increasing to 40 wt.%. For PP-elastomer/carbon black composite, the volume resistivity is 0.64 Ω·cm when the carbon black content is 50 wt.%. However, at the same time, the volume resistivity of PP-elastomer/carbon fiber composite

is 1319 Ω·cm, which is much higher than that of PP-elastomer/carbon black composite. High conductivity is crucial for the current collector materials, and therefore, PP-elastomer/carbon black composite is a more suitable for current collectors. We also prepared PP-elastomer/graphite composite with different graphite content. However, its volume resistivity is even higher than that of PP-elastomer/carbon fiber composite, so the PP-elastomer/graphite composite is not discussed in the present study.

PP-elastomer is a type of amorphous polymers with little or weak crystalline. In general, carbon blacks can only be dispersed in the amorphous phase of the polymer, and the crystalline phase is inaccessible for carbon blacks due to the repulsive force of the lattice. If some strong crystalline phase is introduced into the PP-elastomer, the relative concentration of carbon blacks in the amorphous phase will obviously increase due to the repulsion effect, resulting in the formation of a more complete conductive network in the carbon black rich region [**Figure 3 (a-b)**]. It is expected that the conductivity of the composite is enhanced without increasing the amount of carbon blacks. Here, PP is considered to introduce into the composite, because PP is a high crystalline polymer. Besides, the compatibility between PP and PP-elastomer is very good. PP-elastomer/carbon black composite with 15 wt.% carbon blacks and 85 wt.% polymer (PP+PP-elastomer) is chosen to carry out the investigation. In **Figure 3 (d)**, as expected, the introduction of PP (increasing of PP:PP-elastomer ratio) significantly reduces the volume resistivity of the composite. The volume resistivity sharply declines from 6.18×10^6 Ω·cm to 7410 Ω·cm with PP:PP-elastomer ratio increasing from 0:100 to 20:80, whereas the content of carbon blacks in the composite is unchanged and fixed at 15 wt.%. Only a small amount of PP has a great contribution to the conductivity enhancement.

As discussed above, although the conductivity of PP-elastomer/carbon fiber composite is worse than that of PP-elastomer/carbon black composite, if both carbon black and carbon fiber are simultaneously used, the conductivity of the composite will probably be enhanced further. As shown in **Figure 3 (c)**, this idea comes from the principle that carbon fibers can bridge carbon black particles to form many new conductive paths. This arouses our great curiosity, and therefore, a series of experiments were conducted (**Table 1**). Here, we call this composite with new component as PP-elastomer/PP/carbon black/carbon fiber composite. In **Figure 3 (d)**, because of the content of the conductive fillers (carbon blacks) being low, although the introduction of PP significantly decreased the volume resistivity, the prepared composite is far from meeting the requirements of a high conductivity for the current collectors. Thus, in the following experiments, both the polymer and conductive fillers in the composite are fixed at 50 wt.%, and the PP:PP-elastomer ratio is chosen as 20:80. The volume resistivity of PP-elastomer/PP/carbon black/carbon fiber composite with different carbon fiber:carbon black ratio is shown in **Figure 3 (e)**. A high conductive composite with the volume resistivity at 0.47 Ω·cm is successfully prepared when carbon fiber:carbon black ratio is 20:80. The phenomenon can be interpreted as that carbon blacks form the short-range conductive network, and carbon fibers form the long-range conductive network [**Figure 3 (c)**]. It should be noticed that an upward trend of the volume resistivity is observed when carbon fiber:carbon black ratio is greater than 40:60.

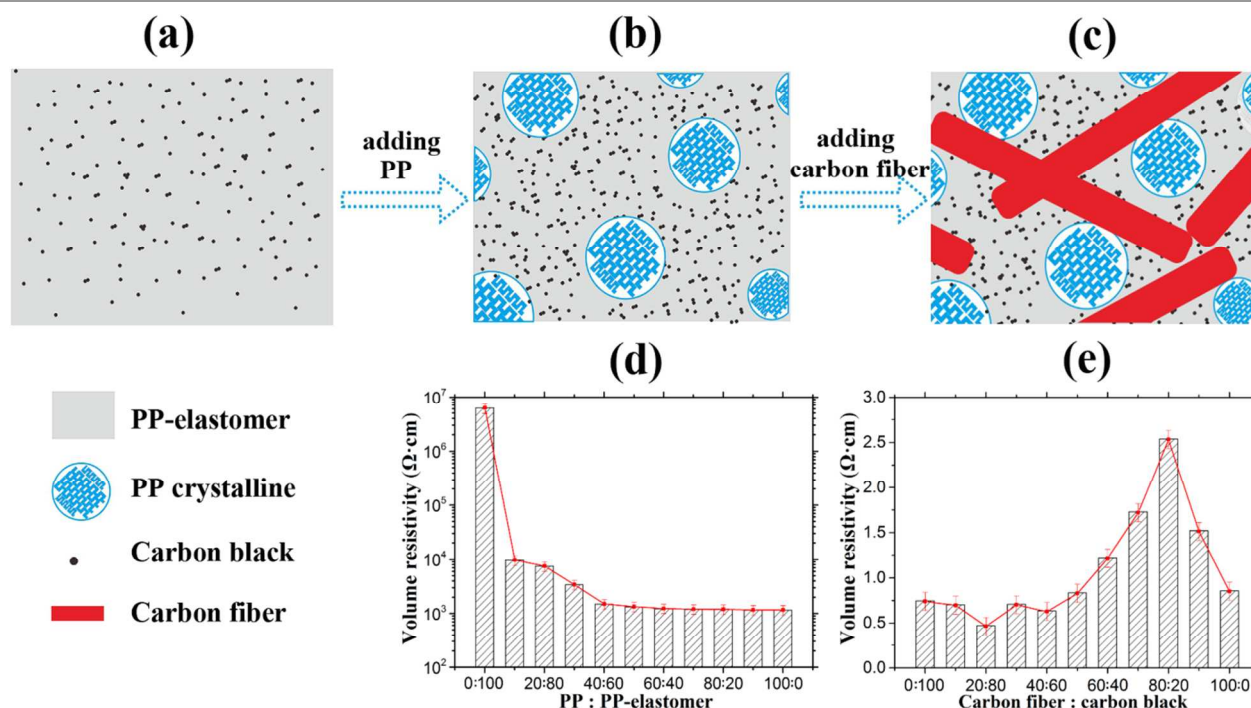


Figure 3. Scheme of the preparation process and the volume resistivity of PP-elastomer composites. (a) PP-elastomer/carbon black composite; (b) PP-elastomer/PP/carbon black composite; (c) PP-elastomer/PP/carbon black/carbon fiber composite; (d) the volume resistivity of PP-elastomer/PP/carbon black composite with different weight ratio of PP:PP-elastomer. The total content of polymer (PP+PP-elastomer) and carbon blacks in composites are fixed at 85 wt.% and 15 wt.%, respectively; (e) the volume resistivity of PP-elastomer/PP/carbon black/carbon fiber composite with different weight ratio of carbon fiber:carbon black. The total content of conductive fillers, PP, and PP-elastomer in composites are fixed at 50 wt.%, 10 wt.%, and 40 wt.%.

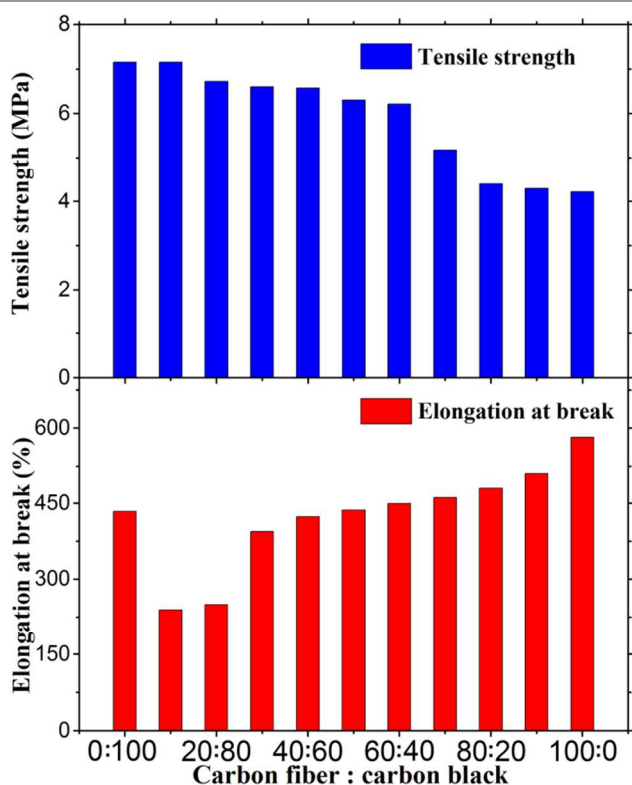


Figure 4. Mechanical properties of PP-elastomer/PP/carbon black/carbon fiber composite with different weight ratio of carbon fiber:carbon black. Total content of conductive fillers is 50 wt.%.

Tensile properties of PP-elastomer/PP/carbon black/carbon fiber composites were measured and illustrated in **Figure 4**. The tensile strength of the composite gradually decreases with the weight ratio of carbon fiber:carbon black increasing. The elongation at break of the composite first decreases with carbon fiber:carbon black ratio increasing from 0:100 to 20:80, and then gradually enhances when the weight ratio is above 30:70. For the case of the weight ratio with 20:80, the tensile strength and the elongation at break are 6.6 MPa and 250%, respectively. Although its elongation at break is relatively low among the prepared composites (**Figure 4**), it is still enough to meet the requirement of current collectors' materials.

The rheology of composites is also concerned by us, and it is critical for producing current collectors by molding. A high pressure capillary rheometer was used to investigate the viscosity of the melts of the PP-elastomer/PP/carbon black/carbon fiber composite at different shear rates. As illustrated in **Figure 5**, composites show a shear thinning behavior, because the viscosity gradually decreases with the shear rate increasing. This indicates that the fluidity of the composites can be enhanced by increasing the shear rate during the current collectors' production, resulting in a good mold filling. It is noticed that the viscosity of the composite with carbon fiber:carbon black ratio of 0:100 decreases significantly with the increase of shear rate, and shows a different trend compared with other composites. The reason is that carbon blacks are ultrafine particulate fillers, which does not affect the rheological behavior of the polymer matrix. The conductive filler of the composite with the ratio of 0:100 are only carbon blacks. Thus, the rheological curve of this composite is similar with that of polymer matrix (PP-elastomer), showing a great shear thinning behavior.

However, the conductive filler of other composites contains carbon fibers. The carbon fiber used here has a large aspect ratio (around 786), which can effectively form a continuous network in the polymer matrix. This continuous network of carbon fibers can stabilize the polymer melt at a high shear rate, resulting in the shear thinning behavior being partly inhibited. In **Figure 5**, it also can be observed that the increase of carbon fiber:carbon black ratio obviously decrease the composites' viscosity at a fixed shear rate, especially when the weight ratio is above 40:60.

PP-elastomer/PP/carbon black/carbon fiber composite with carbon fiber:carbon black ratio of 20:80 is chosen to produce the current collectors, because this composite has highest conductivity, adequate mechanical properties, and good flow property in processing. The current collectors of this composite were prepared using compression molding at a pressure of 10 MPa (200 °C). The single cell and the cell stack of all-vanadium redox flow battery equipped with the composite current collectors were assembled for the following battery performance test.

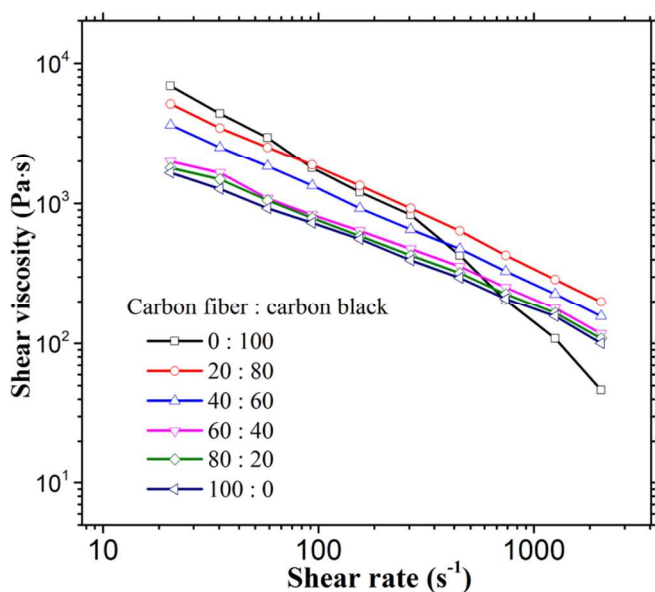


Figure 5. Rheological properties of PP-elastomer/PP/carbon black/carbon fiber composite with different weight ratio of carbon fiber:carbon black at 200 °C.

3.2. Cyclic voltammetry curves

The cyclic voltammograms (CVs) for both current collectors of the graphite material and PP-elastomer/PP/carbon black/carbon fiber composite in 1.5 M $\text{VOSO}_4 + 2.0 \text{ M H}_2\text{SO}_4$ electrolytes are shown in **Figure 6**. For the graphite current collectors [**Figure 6(b)**], there appear two distinct oxidation peaks during the anodic scan at -0.4, and 1.6 V. These two peaks can be attributed to the reactions of $\text{V}^{2+} - \text{e}^- \rightarrow \text{V}^{3+}$ and $\text{VO}_2^+ - \text{e}^- \rightarrow \text{VO}_2^+$, respectively. In the cathodic scan, a strong reduction peak appears at 0.5 V and a weak reduction peak is observed at -0.5 V, which corresponds to the reactions of $\text{VO}_2^+ + \text{e}^- \rightarrow \text{VO}^{2+}$ and $\text{V}^{3+} + \text{e}^- \rightarrow \text{V}^{2+}$, respectively. The vanadium redox peaks occur on graphite current collectors, indicating a strong electrochemical activity of graphite materials for the vanadium ion. By contrast, in **Figure 6(a)**, the PP-elastomer/PP/carbon black/carbon fiber composite only shows a cathodic peak ($\text{VO}_2^+ + \text{e}^- \rightarrow \text{VO}^{2+}$) during the potential scanning range from -1.0 to 2.0 V. This phenomenon

demonstrates that PP-elastomer/PP/carbon black/carbon fiber composite has a low electrochemical activity with vanadium electrolyte. In general, the primary function of current collectors is to transfer electrons of the electrochemical reaction between the anode and the cathode, rather than the electrochemical reaction with electrolytes. From this point of view, the conductive composite is a good alternative for the graphite materials.

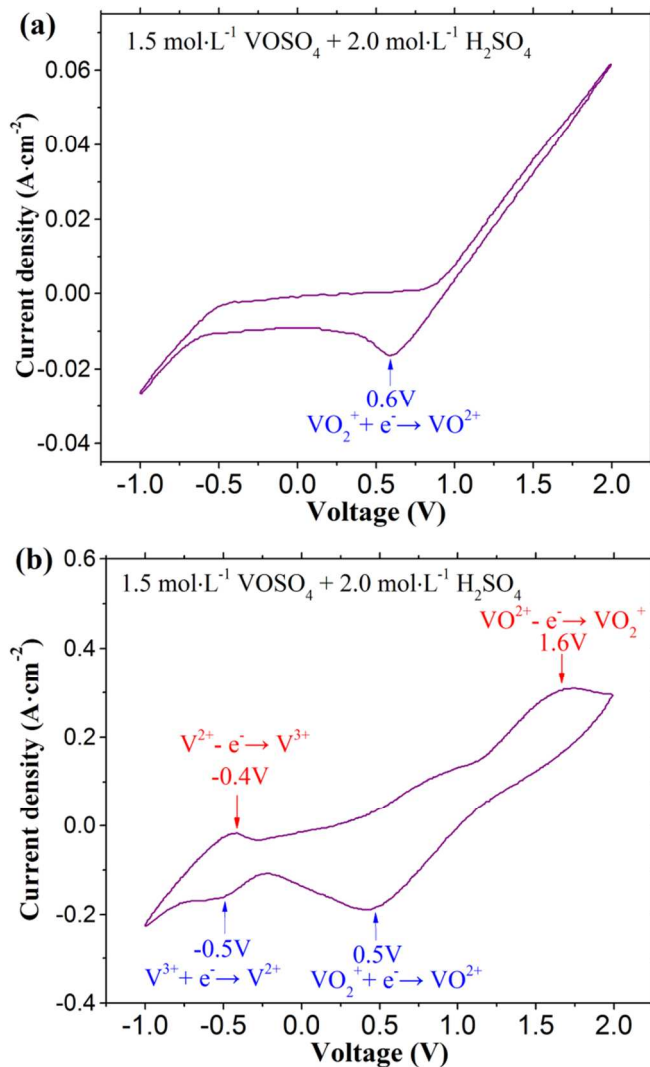


Figure 6. (a) Cyclic voltammetry curves of PP-elastomer/PP/carbon black/carbon fiber composite as current collectors in electrolytes of 1.5 M $\text{VOSO}_4 + 2.0 \text{ M H}_2\text{SO}_4$. (b) Cyclic voltammetry curves of graphite current collectors in electrolytes of 1.5 M $\text{VOSO}_4 + 2.0 \text{ M H}_2\text{SO}_4$. The voltage window of cyclic voltammetry curves is between -1.0 and 2.0 V.

3.3. Stability and the performance of VRB

The galvanostatic charge-discharge data of a single cell with the current density at $70 \text{ mA} \cdot \text{cm}^{-2}$ is illustrated in **Figure 7 (a)**. The performance of the single cell is stability. The average value of the coulombic efficiency (CE) and the voltage efficiency (VE) are 96% and 85% during up to 112 charge-discharge cycles, respectively. At the same time, the energy efficiency (EE) is always above 82%. Therefore, the composite current collectors show a good performance on the single cell for a high current density. In this study, a typical

current density under normal operating conditions is actually $50 \text{ mA}\cdot\text{cm}^{-2}$. For VRB single cell, the current density is intentionally increased to $70 \text{ mA}\cdot\text{cm}^{-2}$. The purpose is to investigate the charge-discharge performance and the energy efficiency at a high current density. It is believed that if the cell has an excellent performance at a high current density, it will be stable and excellent at a lower current density.

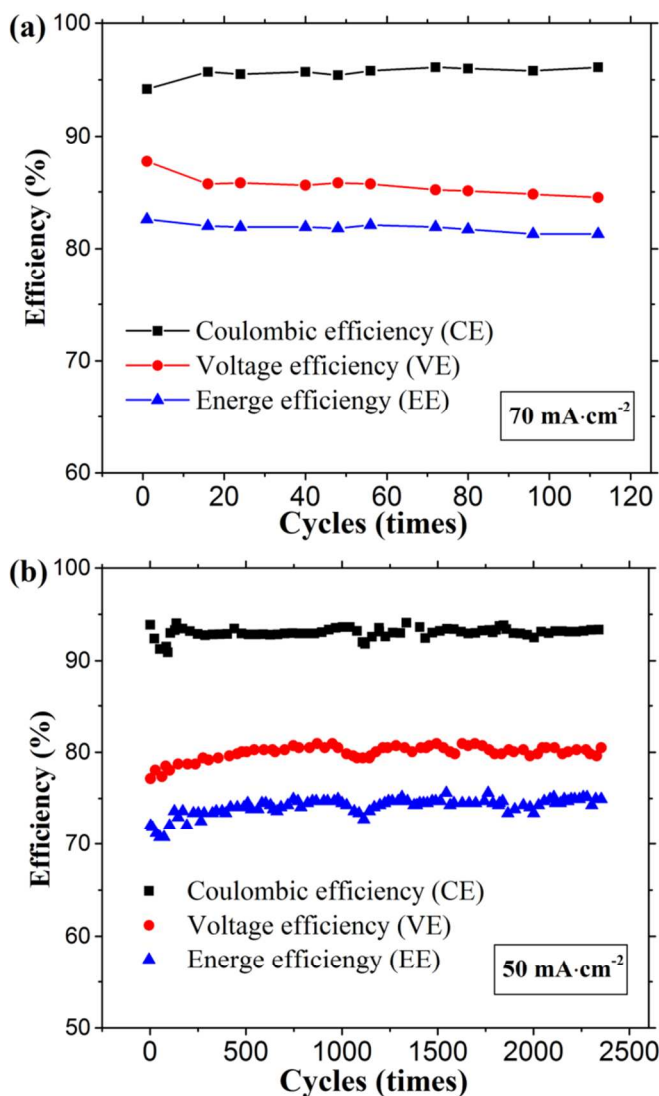


Figure 7. (a) Cycling performance of VRB single cell equipped with current collectors of PP-elastomer/PP/carbon black/carbon fiber composite at a current density of $70 \text{ mA}\cdot\text{cm}^{-2}$. (b) Cycling performance of VRB cell stack equipped with current collectors of PP-elastomer/PP/carbon black/carbon fiber composite at a current density of $50 \text{ mA}\cdot\text{cm}^{-2}$.

The galvanostatic charge-discharge data of the cell stack (composed of five single cells) was further tested with current density at $50 \text{ mA}\cdot\text{cm}^{-2}$ [Figure 7 (b)]. The cell stack of VRB has a more practical value than a single cell due to the requirement of a high effective power for the industrialized storage. To evaluate the stability and the performance of all-vanadium redox flow battery equipped with the composite current collectors under a long-term operating condition, more than 2300 charge-discharge cycles were carried out for the cell stack. As shown in Figure 7 (b), the CE and VE maintain around 93% and 80% during 2300 charge-discharge cycles,

and the EE of the cell stack holds around 75%. It is noticed that the CE and VE of the cell stack are slightly decreased comparing with that of the single cells. This is probably because of the high internal resistance of the cell stack, resulting in a loss increasing of internal energy. Besides, the cell stack easily induces an uneven distribution of the electrolyte, and the generated polarization voltage reduces the battery efficiency. It can be clearly observed that the CE, VE, and EE almost remain constant after being charged and discharged for more than 2300 cycles. The results from the cell stack approve that the all-vanadium redox flow battery equipped the composite current collectors have a good stability and good performance under a long-term operating condition. A typical series of charge-discharge curves of the cell stack are provided in Figure 8.

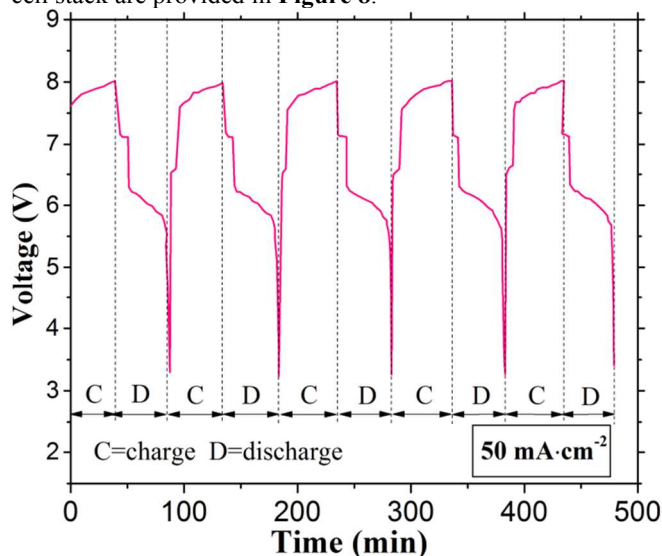


Figure 8. A typical charge-discharge curve of VRB cell stack equipped with current collectors of PP-elastomer/PP/carbon black/carbon fiber composite at a current density of $50 \text{ mA}\cdot\text{cm}^{-2}$.

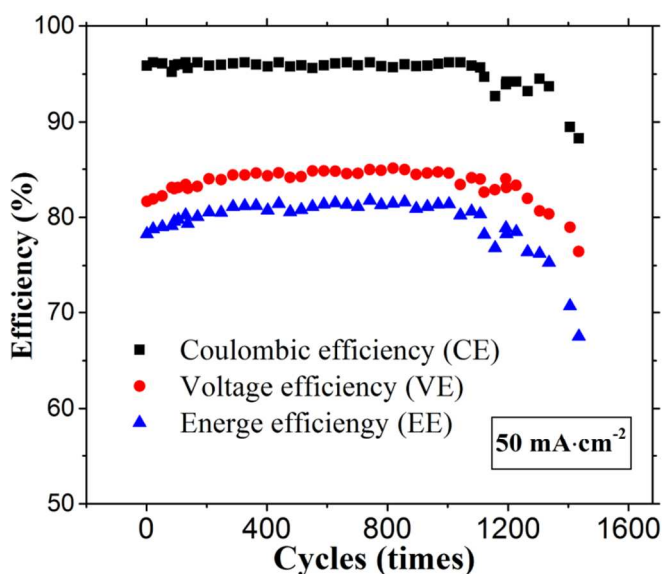


Figure 9. Cycling performance of VRB cell stack equipped with graphite current collectors at a current density of $50 \text{ mA}\cdot\text{cm}^{-2}$.

Figure 9 illustrates the data of the cycling performance of VRB cell stack equipped with graphite current collectors. This is also an experiment under a long-term operating condition, and more than 1600 charge-discharge cycles are carried out. The data of 1450 charge-discharge cycles is shown in **Figure 9**. This is because the cell stack with graphite current collectors showed an obvious failure after 1450 charge-discharge cycles, and we stopped to collect the data. It can be observed that the CE, VE, and EE maintain around 96%, 84% and 80% when the charge-discharge cycles are less than 1200. The CE, VE, and EE of the cell stack with graphite

current collectors are 3%, 4%, and 5% higher than those of the cell stack with composite current collectors. However, an obvious decline of the CE, VE, and EE is observed when charge-discharge cycles are more than 1200. The reason is probably due to the corrosion on graphite current collectors resulting in the electrolyte leakage. In the present study, although the efficiency of the cell stack with graphite current collectors is better than that of composite current collectors, the stability and the performance of the cell stack with graphite current collectors under a long-term operating condition is significantly worse.

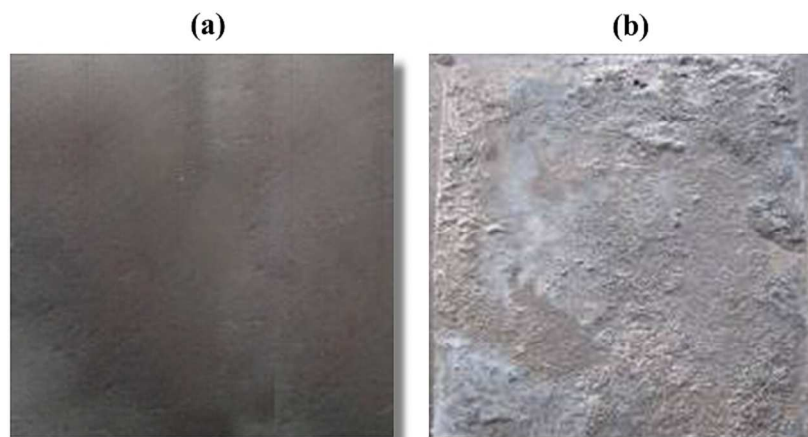


Figure 10. Digital photographs of graphite current collectors of the anode. (a) Before using; (b) After 1600 charge-discharge cycles.

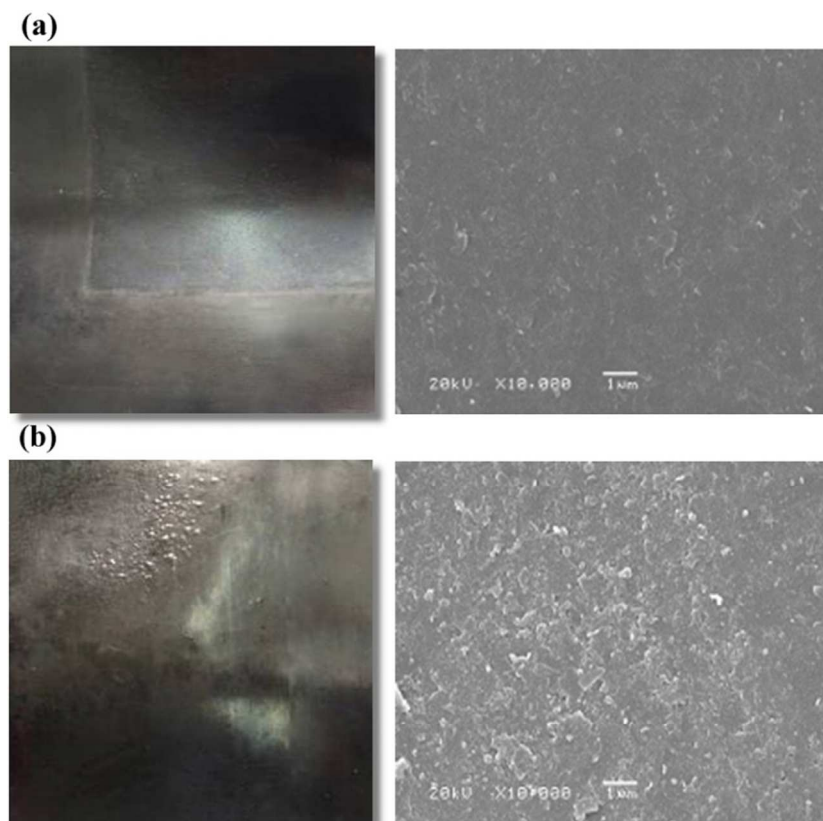


Figure 11. Photographs and SEM images of current collectors of the PP-elastomer/PP/carbon black/carbon fiber composite on the anode. (a) Before using; (b) After more than 2300 charge-discharge cycles.

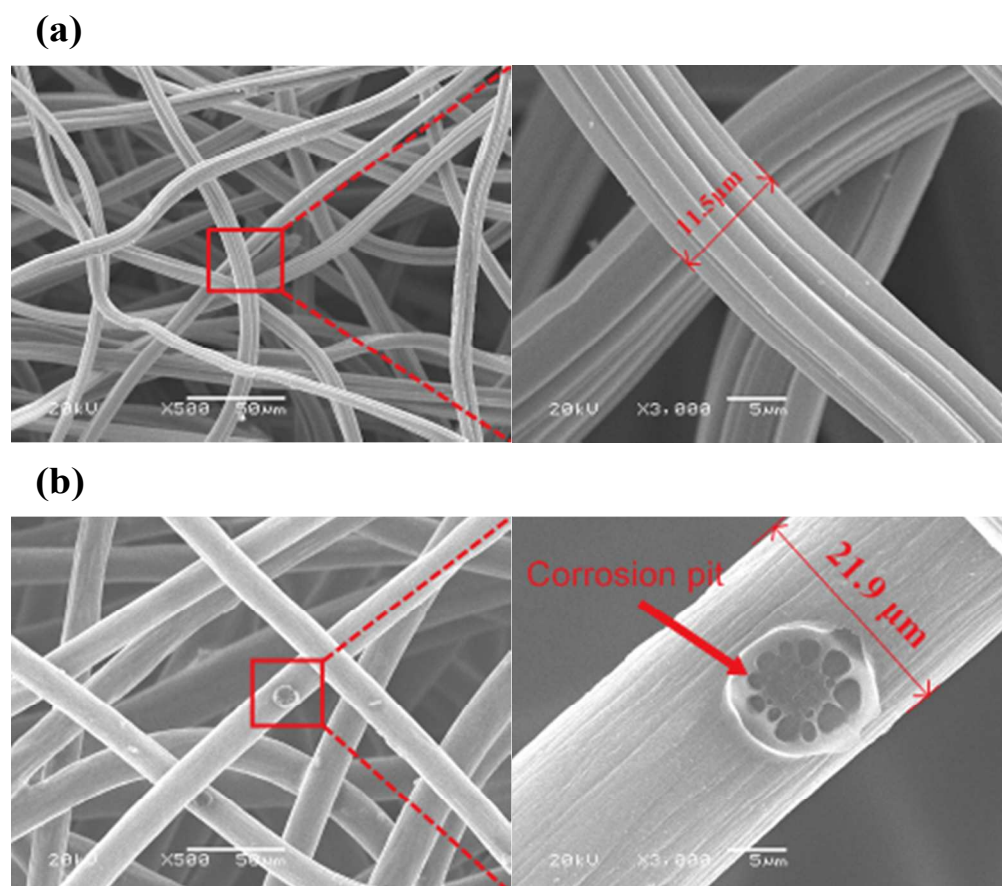


Figure 12. SEM images of the graphite felt on the anode. (a) Before using; (b) After more than 2300 charge-discharge cycles.

3.4. Corrosion of current collectors and the electrode

3.4.1. Graphite current collectors

Several people reported that little corrosion occurred on current collectors of the cathode, while a strong corrosion presented on current collectors of the anode after the death of all-vanadium redox flow battery.³⁹⁻⁴² Figure 10 shows the digital photographs of graphite current collectors on the anode before using and after the death of all-vanadium redox flow battery (1600 charge-discharge cycles) in the present study. A strong corrosion is observed on graphite current collectors of the anode [Figure 10 (b)]. The reason is probably due to the oxygen corrosion of the surface of graphite current collectors, and an obvious etching to the surface and the core takes place.⁴³ The collapse of graphite current collectors is likely to occur after a long-term operation, resulting in the leakage of strongly acidic electrolytes.

3.4.2. Composite current collectors

Digital photographs and SEM images of composite current collectors on the anode before using and after more than 2300 charge-discharge cycles are shown in Figure 11. It should be noticed that the test of the cell stack was artificially cancelled by us after 2300 charge-discharge cycles, other than the death of the battery. Local bubble phenomenon can be observed on the surface of composite current collectors [Figure 11 (b)].

This indicates that acid electrolytes still have a slight corrosion on composite materials after more than 2300 charge-discharge cycles. In contrast, the corrosion resistance of composite materials [Figure 11 (b)] is much better than that of the graphite [Figure 10 (b)]. SEM was employed to characterize the morphology of the surface of the composite current collectors. Comparing with the composite current collectors before using, a rough morphology is observed for the current collectors after more than 2300 charge-discharge cycles, which also indicates the slight corrosion. From the viewpoint of the corrosion resistance, the composite materials prepared in this study are more suitable to produce the current collectors.

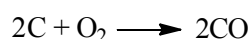
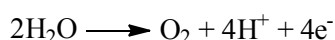
3.4.3. Graphite felt

In all-vanadium redox flow battery, the graphite felt is the electrode which provides reaction sites for electrochemical reactions.⁴⁴ Figure 12 is the SEM images of the graphite felt of all-vanadium redox flow battery equipped with the composite current collectors after more than 2300 charge-discharge cycles. The graphite felt undergoes a significant change in the morphology and size. SEM images on the right are the corresponding enlarged images of the images on the left. Compared with the graphite felt before using, the diameters of the graphite fiber of graphite felt increases from 11.5 μm to 21.9 μm . Meanwhile, some strong

corrosion is clearly observed on the surface of the graphite fiber, showing obviously corrosion holes in **Figure 12 (b)**. Compared to the composites prepared in the present study, the graphite materials are very prone to a strong corrosion in all-vanadium redox flow battery, whether the graphite is used as current collectors or the electrode.

3.4.4. Oxygen corrosion

The oxygen from the anode plays a key role on corrosion to current collectors or the electrode in all-vanadium redox flow battery.⁴³ The oxygen releasing reaction and carbon atom oxidation could happen at a significant rate when a large overpotential is applied. These two reactions are described as follows:⁴²



The oxygen can be easily reacted with carbon atoms, and therefore, both CO and CO₂ gas are generated, resulting in the weight loss of current collectors or the electrode.⁴¹ In general, the graphite contains a large number of unsaturated carbon atoms, whereas the carbon atoms in both PP-elastomer and PP are completely saturated. The oxidation of unsaturated carbon atoms is certainly much faster than that of saturated carbon atoms. This viewpoint can explain the phenomenon that the corrosion resistance of the composite current collectors is much better than that of graphite materials. The oxidation of the unsaturated carbon atoms is probably a multi-step process. As shown in **Figure 13**, the unsaturated carbon atoms are firstly oxidized to oxygen-containing groups, such as C–OH and C=O, and then is transformed into COOH. Finally, CO and CO₂ gas is released, resulting in the loss of the unsaturated carbon atoms.

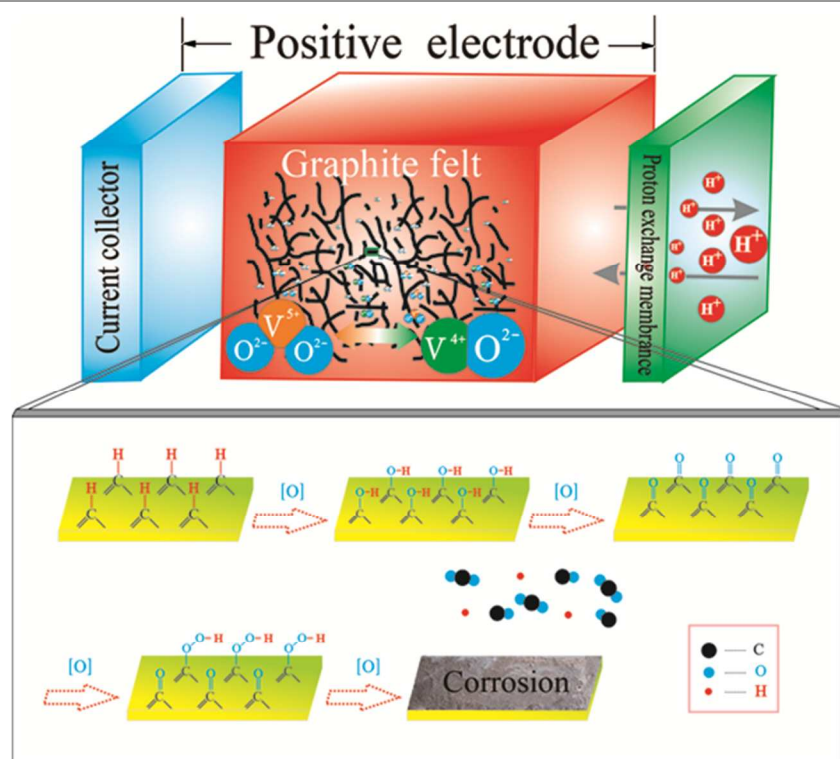


Figure 13. Scheme of the corrosion mechanism of positive graphite felt.

4. Conclusions

PP-elastomer/PP/carbon black/carbon fiber composite with a high conductivity and good mechanical properties was successfully prepared for current collectors materials in all-vanadium redox flow battery. The volume resistivity of the prepared composite was 0.47 Ω·cm. Its tensile strength and elongation at break were 6.6 MPa and 250%, respectively. In addition, good flow property in processing makes this

composite has the potential on mass industrial production of current collectors.

The single cell and the cell stack of all-vanadium redox flow battery equipped with the composite current collectors were assembled for battery tests, including cyclic voltammetry, long-term performance, long-term stability, and the oxidation corrosion. The results of cyclic voltammetry indicated that the composite current collectors only showed a cathodic peak compared to the graphite current collectors. To evaluate the stability and the performance of the cell stack under a

long-term operating condition, tests with more than 2300 charge-discharge cycles were carried out. The CE and VE of the cell stack maintained around 93% and 80% during 2300 charge-discharge cycles, and the EE hold around 75%. The results approved that the all-vanadium redox flow battery equipped the composite current collectors had a good stability and excellent performance.

After a long-term operation, the composite current collectors only presented a slight corrosion on the surface, whereas the severe corrosion was observed on the graphite current collectors and the graphite felt. This approved the composite materials prepared in this study are more suitable to produce the current collectors. The corrosion resistance of composite materials is much better than that of the graphite, and the mechanism was also discussed.

Acknowledgements

This work was supported by the National Natural Science Foundation of China (Grant No. 51473104, 51003066), State Key Laboratory of Polymer Materials Engineering (Grant No. sklpm2014-3-06), and the Outstanding Young Scholars Foundation of Sichuan University (Grant No. 2011SCU04A13).

Notes and references

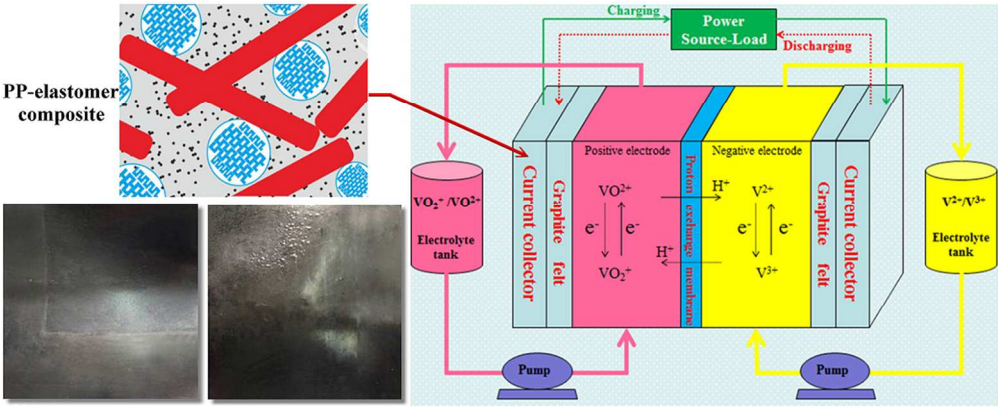
^a State Key Laboratory of Polymer Materials Engineering of China, Polymer Research Institute, Sichuan University, Chengdu 610065, China.

^b Technology Research Center of Polymer Materials Engineering of Tai'an, Longteng Polymer Materials Co., Ltd., Tai'an 271000, China

*Corresponding author. Tel.: +86-28-85402601; Fax: +86-28-85402465; E-mail address: zhoutaopoly@scu.edu.cn (T. Zhou) or amzhang215@vip.sina.com (A. Zhang)

1. A. Tang, J. McCann, J. Bao and M. Skyllas-Kazacos, *J. Power Sources*, 2013, **242**, 349-356.
2. M. Skyllas-Kazacos, M. Chakrabarti, S. Hajimolana, F. Mjalli and M. Saleem, *J. Electrochem. Soc.*, 2011, **158**, R55-R79.
3. T. Shigematsu, *SEI Technical Review*, 2011, **73**, 5-13.
4. P. Alotto, M. Guarnieri and F. Moro, *Renew. Sust. Energ. Rev.*, 2014, **29**, 325-335.
5. A. Z. Weber, M. M. Mench, J. P. Meyers, P. N. Ross, J. T. Gostick and Q. Liu, *J. Appl. Electrochem.*, 2011, **41**, 1137-1164.
6. P. Leung, X. Li, C. P. de León, L. Berlouis, C. J. Low and F. C. Walsh, *RSC Adv.*, 2012, **2**, 10125-10156.
7. S.-H. Shin, S.-H. Yun and S.-H. Moon, *RSC Adv.*, 2013, **3**, 9095-9116.
8. M. H. Chakrabarti, S. Hajimolana, F. S. Mjalli, M. Saleem and I. Mustafa, *Arab. J. Sci. Eng.*, 2013, **38**, 723-739.
9. W. J. Dai, Y. Shen, Z. H. Li, L. H. Yu, J. Y. Xi and X. P. Qiu, *J. Mater. Chem. A*, 2014, **2**, 12423-12432.
10. S. T. Senthilkumar, R. K. Selvan, N. Ponpandian, J. S. Melo and Y. S. Lee, *J. Mater. Chem. A*, 2013, **1**, 7913-7919.
11. N. F. Yan, G. R. Li and X. P. Gao, *J. Mater. Chem. A*, 2013, **1**, 7012-7015.
12. E. Sum and M. Skyllas-Kazacos, *J. Power Sources*, 1985, **15**, 179-190.
13. M. Skyllas - Kazacos and F. Grossmith, *J. Electrochem. Soc.*, 1987, **134**, 2950-2953.
14. M. Rychcik and M. Skyllas-Kazacos, *J. Power Sources*, 1988, **22**, 59-67.
15. M. Kazacos and M. Skyllas-Kazacos, *J. Electrochem. Soc.*, 1989, **136**, 2759-2760.
16. D. You, H. Zhang and J. Chen, *Electrochim. Acta.*, 2009, **54**, 6827-6836.
17. M. S. J. Jung, J. Parrondo, C. G. Arges and V. Ramani, *J. Mater. Chem. A*, 2013, **1**, 10458-10464.
18. S. Yun, J. Parrondo and V. Ramani, *J. Mater. Chem. A*, 2014, **2**, 6605-6615.
19. H. P. Zhang, S. S. Liang, B. P. Sun, X. J. Yang, X. Wu and T. Yang, *J. Mater. Chem. A*, 2013, **1**, 14476-14479.
20. H. Z. Zhang, C. Ding, J. Y. Cao, W. X. Xu, X. F. Li and H. M. Zhang, *J. Mater. Chem. A*, 2014, **2**, 9524-9531.
21. C. Ding, H. Zhang, X. Li, T. Liu and F. Xing, *J. Phys. Chem. Lett.*, 2013, **4**, 1281-1294.
22. S. H. Zhang, B. G. Zhang, D. B. Xing and X. G. Jian, *J. Mater. Chem. A*, 2013, **1**, 12246-12254.
23. S. H. Zhang, B. G. Zhang, G. F. Zhao and X. G. Jian, *J. Mater. Chem. A*, 2014, **2**, 3083-3091.
24. M. Chakrabarti, N. Brandon, S. Hajimolana, F. Tariq, V. Yufit, M. Hashim, M. Hussain, C. Low and P. Aravind, *J. Power Sources*, 2014, **253**, 150-166.
25. A. Parasuraman, T. M. Lim, C. Menictas and M. Skyllas-Kazacos, *Electrochim. Acta.*, 2013, **101**, 27-40.
26. C. Ponce-de-León, G. Reade, I. Whyte, S. Male and F. Walsh, *Electrochim. Acta.*, 2007, **52**, 5815-5823.
27. B. Li, M. Gu, Z. Nie, Y. Shao, Q. Luo, X. Wei, X. Li, J. Xiao, C. Wang and V. Sprenkle, *Nano Lett.*, 2013, **13**, 1330-1335.
28. M. Park, Y.-j. Jung, J. Kim, H. i. Lee and J. Cho, *Nano Lett.*, 2013, **13**, 4833-4839.
29. B. Sun and M. Skyllas-Kazacos, *Electrochim. Acta.*, 1992, **37**, 1253-1260.
30. S. Zhong, M. Kazacos, R. Burford and M. Skyllas-Kazacos, *J. Power Sources*, 1991, **36**, 29-43.
31. V. Haddadi-Asl, M. Kazacos and M. Skyllas-Kazacos, *J. Appl. Electrochem.*, 1995, **25**, 29-33.
32. V. Haddadi-Asl, M. Kazacos, M. S. Kazacos and S. Zhong, US Patent No. 5,665,212, Sept, 1997.
33. P. Leung, C. Ponce de León, C. Low and F. Walsh, *Electrochim. Acta.*, 2011, **56**, 2145-2153.
34. A. Brungs, V. Haddadi-Asl and M. Skyllas-Kazacos, *J. Appl. Electrochem.*, 1996, **26**, 1117-1123.
35. B. Caglar, P. Fischer, P. Kauranen, M. Karttunen and P. Elsner, *J. Power Sources*, 2014, **256**, 88-95.
36. V. Haddadi - Asl, M. Kazacos and M. Skyllas - Kazacos, *J. Appl. Polym. Sci.*, 1995, **57**, 1455-1463.
37. X. Teng, J. Dai, J. Su, Y. Zhu, H. Liu and Z. Song, *J. Power Sources*, 2013, **240**, 131-139.

38. W. Zhang, A. A. Dehghani-Sanij and R. S. Blackburn, *J. Mater. Sci.*, 2007, **42**, 3408-3418.
39. S. Rudolph, U. Schröder, I. Bayanov and G. Pfeiffer, *J. Electroanal. Chem.*, 2013, **709**, 93-98.
40. H. Liu, Q. Xu and C. Yan, *Electrochem. Commun.*, 2013, **28**, 58-62.
41. A. Di Blasi, N. Briguglio, O. Di Blasi and V. Antonucci, *Appl. Energ.*, 2014, **125**, 114-122.
42. H. Liu, Q. Xu, C. Yan and Y. Qiao, *Electrochim. Acta.*, 2011, **56**, 8783-8790.
43. B. Avasarala, R. Moore and P. Haldar, *Electrochim. Acta.*, 2010, **55**, 4765-4771.
44. Z. Yang, J. Zhang, M. C. Kintner-Meyer, X. Lu, D. Choi, J. P. Lemmon and J. Liu, *Chem. Rev.*, 2011, **111**, 3577-3613.



111x45mm (271 x 271 DPI)

PP-elastomer composite for VRB current collector is prepared, which has low volume resistivity, good mechanical properties, and good corrosion resistance.